BULLETIN OF THE EARTHQUAKE
RESEARCH INSTITUTE
Vol. 44 (1966), pp. 1519–1535

73. *Studies of the Thermal State of the Earth. The 19th Paper: Heat-Flow Measurements in the Northwestern Pacific.*

By Victor VACQUIER*, Seiya UYEDA**, Masashi YASUI***
John SCLATER*, Charles CORRY* and Teruhiko WATANABE.****

(Read June 28, 1966.—Received Sept. 30, 1966.)

Abstract

Sixty-five new heat-flow measurements were made in the northwestern Pacific off Japan during the ZETES Expedition of R/V ARGO of Scripps Institution of Oceanography, as a part of the US-Japan Cooperative Science Program. The results show that the NW Pacific Basin, including the NW Pacific Rise and Emperor Seamounts, has uniform and slightly sub-normal heat-flow, the average being $1.15 \pm 0.37 \times 10^{-6}$ cal/cm^2 sec. Higher heat-flow values were obtained on crossing the Izu-Mariana (Bonin) Arc. The Shikoku Basin does not appear to be a consistently high heat-flow area. Combined with the existing heat-flow values in and around Japan, present data seem to delineate a fairly complete pattern of heat-flow in an island arc area. For the first time several *in situ* measurements of the thermal conductivity of the bottom were made. Ten such measurements indicated that *in situ* value tends to be about 20% higher than the conventional measurements. This discrepancy requires to be thoroughly investigated, because if it is substantiated, it would affect all values previously measured in the oceans.

1. Introduction

Although there are about 2,000 oceanic heat-flow stations, the northwestern Pacific area has had only a sparse distribution of heat-flow values except for the area very close to the Japanese Islands (Lee and Uyeda, 1965). The land of Japan (Uyeda and Hôrai, 1964) and the Japan Sea (Yasui and Watanabe, 1965 and Yasui et al., 1966, b) have been well

* Marine Physical Laboratory, Scripps Institution of Oceanography, La Jolla, California, U.S.A.
** Earthquake Research Institute and Geophysical Institute, University of Tokyo.
*** Maizuru Marine Observatory.
**** Graduate School, University of Tokyo.

investigated geothermally. It has been shown that there is a definite zonal distribution of heat-flow in the Japan arc area, i.e. heat-flow is low in the Pacific-side of the arc and high in both the continent-side of the arc and in the Japan Sea. It was considered, therefore, that the heat-flow measurement off the Japanese Islands in the Pacific Basin would be of great significance in clarifying the tectonics of the island arc.

A joint program of heat-flow survey in the northwestern Pacific was taken up by the Scripps Institution of Oceanography, University of California and University of Tokyo, Japan Meteorological Agency, and Maritime Safety Agency of Japan and a cooperative survey was made aboard the Scripps research vessel ARGO on her ZETES Expedition in early 1966. The present paper reports the results of heat-flow observations made during this expedition.

2. Heat-flow measurements

Fig. 1 shows the ship's track and the localities of heat-flow stations. On the first leg the ship departed Hakodate on April 5, 1966 and returned to Hakodate, on May 2, after making a loop via the Northwest Pacific Rise at about 33°N, 158°E and Dzingu Seamount of the Emperor Seamount Ridge at about 40°N, 170°E. The track made one crossing of the Japan Trench and three crossings of the Kuril Trench. Thirty-nine heat-flow stations were taken on the first leg.

The second leg of the expedition went from Hakodate (May 6) to Tokyo (May 26). The ship made a crossing over the Japan Trench and sailed southward along 148°E to 27°N. Along the 27°N parallel a crossing of the Izu-Bonin (Mariana) Trench and Arc was made. Twenty-eight heat-flow stations were taken on this leg.

The measurement of the thermal gradient was made by both the Scripps instrument and the Japanese instrument. The former instrument is essentially a modified version of the instrument described by von Herzen et al., (1962). One of the important improvements of the instrument is that the present one has the capability of conducting the *in situ* measurement of thermal conductivity by the needle method of von Herzen and Maxwell (1959). The needle is carried by a body sliding on the temperature gradient probe. This device will be fully described elsewhere. The other improvements are that the gradient is measured at two vertical intervals and the temperature of the water is also measured by a thermistor on top of the instrument case. The Japanese instrument is of the type described earlier (Uyeda et al., 1961). It re-

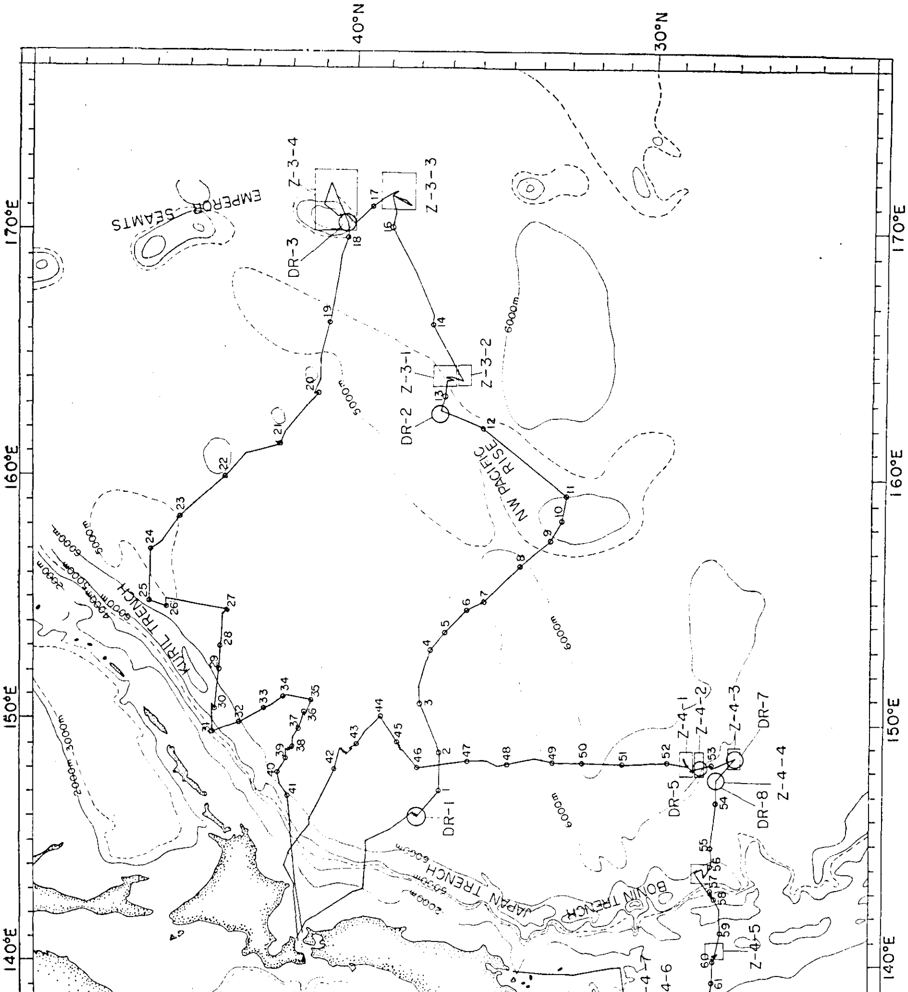

Fig. 1. The track of the R/V Argo in legs III and IV of the ZETES Expedition. Numbers attached to stations are heat-flow station numbers. Z-3-1, etc. are seamounts surveyed and DR-1, etc. are dredge stations.

Table 1. Heat-flow data of ZETES Expedition

Station Number	Position Coordinate		Depth (m)	Thermal Gradient[1]				K[2]	Q[3]	K_i[2]	Q_i[3]	Tilt[4]	Penetration[5]	Inst.[6]
	Latitude	Longitude		U-L	M-L	U-M	Average							
1	37-15 N	147-00 E	5710	0.50	0.50		0.50	1.9 a	1.0			0-15	F	J
2	37-17 N	148-33 E	5733	0.55	0.53		0.54	1.9 a	1.0			0-15	F	J
3	37-55 N	150-32.2E	5766		0.52		0.52	1.76 n	0.92			0-15	P100 cm	J
4	37-38.1N	152-50 E	5811	0.55	0.59		0.57	1.9 a	1.1			0-15	F	J
5	37-07.5N	153-31 E	5796	0.51	0.53		0.52	1.9 a	1.0			0-15	F	J
6	36-22 N	154-26 E	5677	0.48	0.51		0.50	1.9 a	1.0			0-15	P.P.O.	J
7	35-48 N	154-45 E	5511	0.62	0.64	0.59	0.63	1.9 a	1.2			0-15	F	S
8	34-38 N	156-16 E	5449	0.52	0.53		0.53	1.9 a	1.0			0-15	F	J
9	33-35.5N	157-18.5E	4767	0.52	0.53	0.51	0.53	1.9 a	1.0			0-15	F	S
10	33-15 N	158-02 E	3041	0.41	0.48	0.34	0.41	2.04 n	0.84			0-15	F	S
11	33-03.5N	159-07 E	3422	0.46	0.42	0.49	0.45	1.9 a	0.9			0-15	F	S
12	35-50 N	161-51 E	4517	0.50	0.50	0.50	0.50	1.9 a	1.0			0-15	F	S
13	37-08 N	163-10 E	4032	0.49	0.48	0.44	0.46	1.9 a	0.9			0-15	F	S
14	37-34 N	166-03.5E	5020	0.60	0.56		0.58	1.9 a	1.1			0-15	F	J
15	33-08 N	168-05 E	5458	0.58			0.58	1.9 a	1.1			0-15	F	S
16	38-49.8N	169-58.5E	6079					No Penetration						
17	39-39.5N	170-51 E	6237	0.77	0.74	0.76	0.75	1.64 n	1.2			0-15	F	S
18	40-17 N	169-39 E	5617	0.48	0.50		0.49	1.8 a	0.9			0-15	F	J
19	40-44.5N	166-10.0E	5468	0.62	0.62	0.60	0.61	1.8 a	1.1			0-15	F	S
20	41-10 N	168-18.0E	5565	0.68	0.67	0.67	0.67	1.8 a	1.2			0-15	F	S

(to be continued)

Table 1. (continued)

Station Number	Position Coordinate		Depth (m)	Thermal Gradient[1]				K[2]	Q[3]	K_i[2]	Q_i[3]	Tilt[4]	Penetration[5]	Inst.[6]
	Latitude	Longitude		U-L	M-L	U-M	Average							
21	42-17 N	161-11 E	5370	0.64	0.63	0.64	0.64	1.8 a	1.1			0-15	F	S
22	43-53.5N	159-45 E	5487	0.66	0.68	0.62	0.67	1.8 a	1.2			0-15	F	S
23	45-15.5N	158-07.0E	4701	0.71	0.71	0.68	0.70	1.95 n	1.37			0-15	F	S
24	46-06.0N	156-49.0E	4876	0.89	0.72		0.72	1.9 a	1.4	2.42	2.1	15-30	P165 cm	S
25	46-06.0N	154-41 E	5312	0.78	0.795		0.79	1.9 a	1.5			0-15	F	J
26	45-38.0N	154-28.0E	4978	0.79	0.70		0.75	1.84 n	1.37			0-15	F	J
27	43-53.5N	154-18.0E	5365		0.84		0.84	1.7 a	1.4			0-15	F	J
28	44-02.0N	152-53.0E	5224	0.62	0.58		0.60	1.7 a	1.0			0-15	F	J
29	44-06.0N	151-55.5E	5682	1.3	1.3		1.3	1.7 a	(2.2)			30-	P 50 cm	S
30	44-14.0N	150-14.5E	7469	0.48	0.36		0.42	1.7 a	0.6			30-	P140 cm	S
31	44-18.5N	149-14.5E	4308	0.41	0.42		0.42	1.62 n	0.68			15-30	P189 cm	S
32	43-35.0N	149-42.0E	6951	0.70	0.69	0.72	0.70	1.8 a	1.3			0-15	F	S
33	42-47.0N	150-16.0E	4573	0.58	0.56	0.55	0.55	1.8 a	1.0			0-15	F	S
34	42-10.8N	150-51.5E	5032	0.61	0.63	0.56	0.59	1.8 a	1.1			0-15	F	S
35	41-17.0N	150-38.0E	5251	0.71	0.80	0.63	0.71	1.8 a	1.3			0-15	F	S
36	41-30.0N	150-00.0E	5165	0.63	0.60	0.66	0.63	1.8 a	1.1			0-15	F	S
37	41-41.0N	149-31 E	5333	0.68	0.61	0.77	0.69	1.8 a	1.2			0-15	F	S
38	41-55.0N	148-43.0E	5475	0.29	0.29	0.29	0.29	2.14 n	0.63			0-15	F	S
39	42-03 N	148-24 E	5663	0.50	0.44	0.50	0.47	1.8 a	0.9			0-15	F	S
40	42-23 N	142-42.0E	6927	Topography too rough to attempt station										

(to be continued)

Table 1. (continued)

Station Number	Position Coordinate		Depth (m)	Thermal Gradient[1]				K[2]	Q[3]	K_i[2]	Q_i[3]	Tilt[4]	Penetration[5]	Inst.[6]
	Latitude	Longitude		U-L	M-L	U-M	Average							
41	42-02 N	146-46 E	7323	0.53	0.31	0.67	0.49	1.8 a	0.9			0-15	F	S
42	40-33.0N	148-02.0E	5327	0.58	0.52	0.63	0.58	1.9 a	1.1	1.92	1.11	0-15	F	S
43	39-56 N	149-05 E	5590	0.58	0.54	0.64	0.59	1.9 a	1.1	2.14	1.26	0-15	F	S
44	39-15.5N	150-10.0E	5389	0.57	0.55	0.56	0.56	1.9 a	1.1	2.20	1.22	0-15	F	S
45	38-34.0N	149-07 E	5619	0.51	0.51	0.50	0.51	1.9 a	1.0			0-15	F	S
46	37-59.2N	148-09.0E	5675	0.63	0.60	0.66	0.62	1.9 a	1.2			0-15	F	S
47	36-18.5N	148-24.5E	5772	0.55	0.53	0.60	0.56	1.9 a	1.1	2.32	1.30	0-15	F	S
48	35-01.0N	148-20.5E	6004	0.70			0.70	1.9 a	1.3			0-15	F	J
49	33-30 N	148-23 E	6265	0.56	0.50	0.62	0.56	1.9 a	1.1			0-15	F	S
50	32-25.3N	148-20.0E	5762	0.53	0.49	0.61	0.55	1.9 a	1.0			0-15	F	S
51	31-05.0N	148-21.0E	6184	0.53	0.53	0.55	0.54	1.9 a	1.0	2.73	1.47	0-15	F	S
52	29-30.0N	148-25.0E	6204	0.58	0.59	0.58	5.58	1.9 a	1.1			0-15	F	S
53	27-51.0N	148-21.0E	5841	0.50	0.58		0.58	1.9 a	1.1			30-	P 99cm	S
54	27-42.0N	146-46.0E	5790	0.60	0.57	0.61	0.59	1.86 n	1.10	2.55	1.50	0-15	F	S
55	27-53.0N	144-51.0E	5558	0.57	0.52		0.55	1.9 a	.1.0			0-15	F	J
56	57-53.0N	144-06.0E	6179	0.72	0.75	0.71	0.73	1.9 a	1.4	2.66	1.94	0-15	F	S
57	27-56.5N	143-03 E	3372	0.16	0.32		0.32	1.9 a	0.6	2.64	0.93	30-	P133 cm	S
58	27-47.5N	142.45.0E	2737	0.20	0.20		0.20	1.9 a	0.4			30-	P110 cm	S
59	27-28.5N	141-24.0E	4116	0.63	0.70		0.67	1.9 a	1.3	2.48	1.74	30-	P101 cm	S

(to be continued)

Table 1. (continued)

Station Number	Position Coordinate		Depth (m)	Thermal Gradient[1]				K[2]	Q[3]	K_i[2]	Q_i[3]	Tilt[4]	Penetration[5]	Inst.[6]
	Latitude	Longitude		U-L	M-L	U-M	Average							
60	27-48.5N	140-09.0E	3704	0.90	1.02		0.96	2.0 a	0.9	2.23	2.14	15-30	P157 cm	S
61	27-51.0N	139-20.2E	3730	0.14	0.18	0.10	0.14	2.0 a	0.3	2.55	0.36	0-15	F	S
62	27-59.0N	138-11.1E	4635		1.60		1.60	2.0 a	3.2			15-30	P190 cm	S
63	27-51.0N	137-08 E	4759	0.14	0.15		0.14	2.0 a	0.3			15-30	P108 cm	S
64	28-23.5N	136-16 E	4519	0.06	0.10	-0.01	0.05	2.07 n	0.11			0-15	F	S
65	29-11.0N	136-43.0E	4485	0.42	0.55	0.29	0.42	2.1 a	0.9			0-15	F	S
66	29-48 N	136-52.5E	4475	0.17	0.23	0.12	0.17	2.1 a	0.4			0-15	F	S
67	30-22 N	137-27.5E	4203	0.94	0.98	0.93	0.95	2.1 a	2.0			0-15	F	S
68	30-41 N	138-45 E	2171	0.04	0.38	-0.25	0.38	2.1 a	0.8			0-15	F	S
69	31-10 N	139-52 E	2107	Station abandoned—Fast current										
70	29-37 N	174-06 E	4970	0.36	0.33	0.38	0.36	2.1 a	0.6			0-15	F	S
71	25-15 N	164-08 E	4943	0.61	0.57	0.61	0.59	2.05 n	1.21			0-15	F	S
72	24-53.5N	163-21 E	4970	0.54	0.92	0.17	0.54	2.1 a	1.93			0-15	F	S
37	24-32 N	162-36.5E	4930	0.53	0.50	0.57	0.53	2.1 a	1.1			0-15	F	S

Legeneds to Table 1.

1) Thermal gradient in 10^{-3}°C/cm: U-L, gradient between the Upper and Lower thermistors: M-L, between the Middle and Lower thermistors; U-M, between the Upper and Middle thermistors.
2) Thermal conductivity in 10^{-3} cal/cm sec °C. a, estimated value. *n*, value by conventional measurement.
3) Heat-flow in 10^{-6} cal/cm^2 sec.
4) Tilt in degrees of arc.
5) F, full penetration. P, partial penetration. P.P.O., partial pull out.
6) Instrument: J=Japanese instrument, S=Scripps instrument.

cords two temperature gradients.

Because of lack of time, coring for thermal conductivity measurement was made only occasionally. On the first leg the thermal conductivity was measured on seven gravity cores and once *in situ*. On the second leg it was measured on four gravity cores and nine times *in situ*. For the stations where coring was not made, conductivity was estimated from the values of the nearest stations where it was measured. *In situ* values

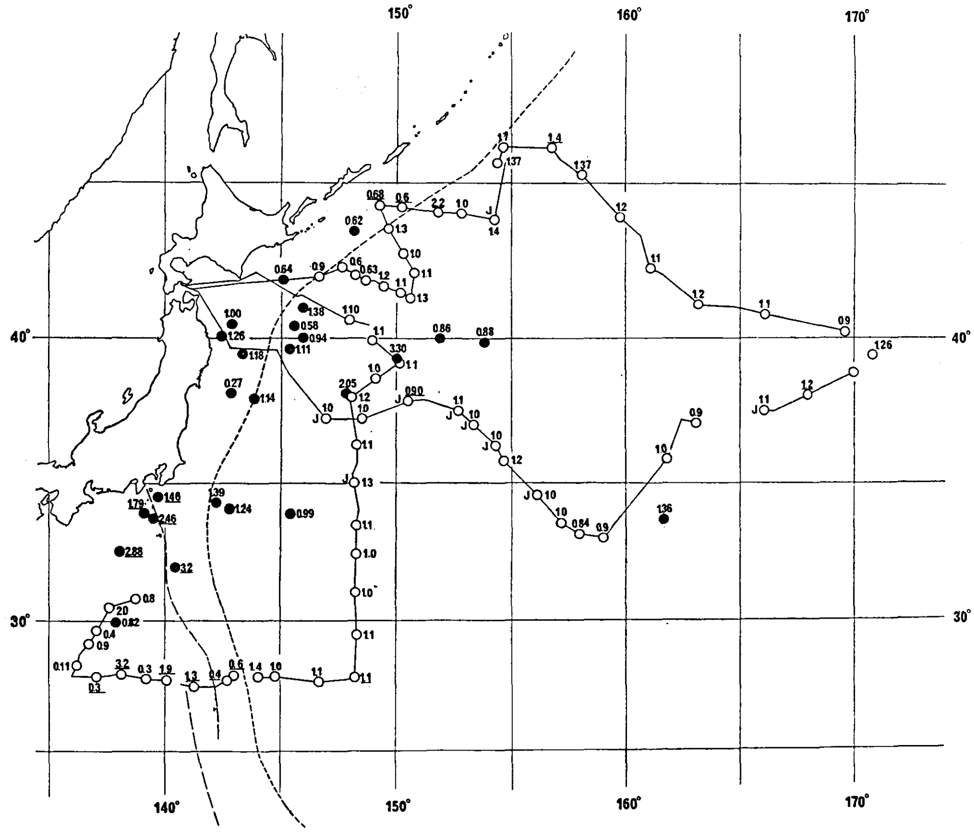

Fig. 2. Heat-flow values in the northwestern Pacific.
Black circles····Previous stations
Hollow circles···ZETES stations
Dotted line······Trench axis
Broken line ·····Axis of Izu-Bonin Arc

Stations with thermal conductivity measured on core sample are indicated by two figures after the decimal point, and stations with estimated conductivity by one figure after the decimal point.

Stations with partial penetration are underlined.

Stations with *J* were taken by the Japanese instrument.

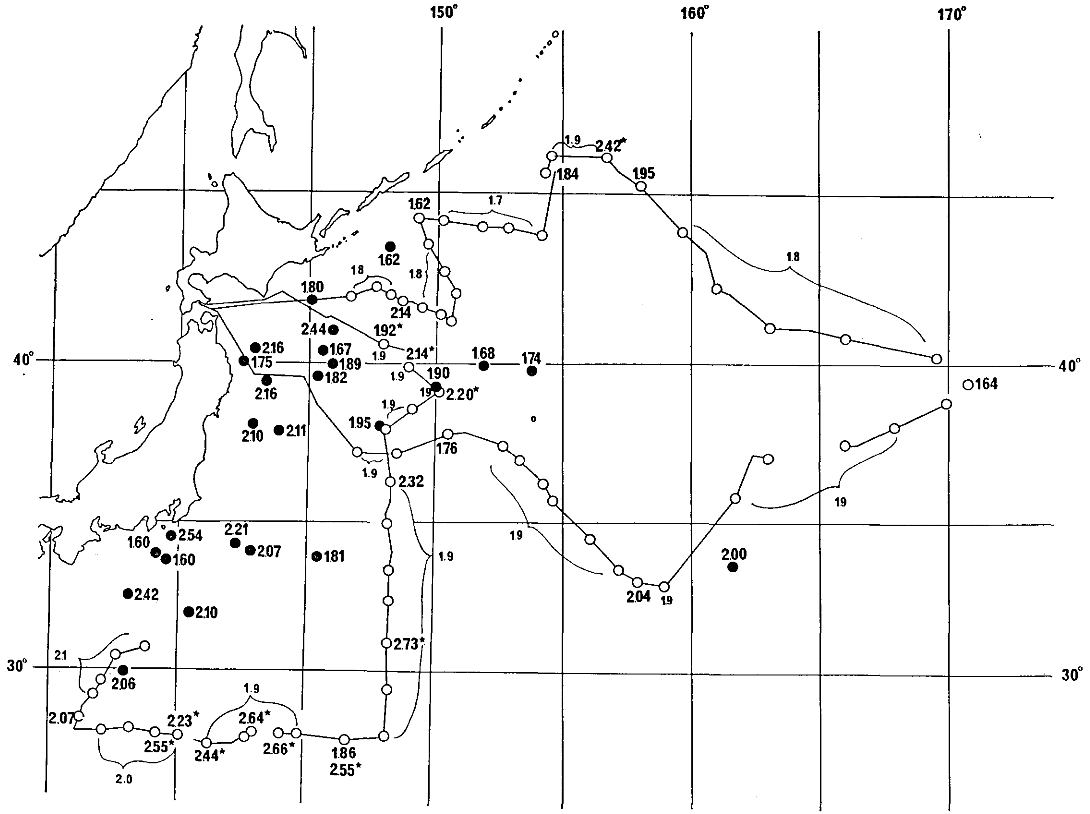

Fig. 3. Thermal conductivity of bottom sediments.

Black circles···Previous measurements Hollow circles···ZETES stations

Two figures after the decimal point are used for measured values, and one figure after the decimal point for estimated values. Value with an asterisk are in situ measurements (K_i).

were disregarded in the present paper: the reason for this will be given later.

The results of the heat-flow measurements are summarized in Table 1 and in Fig. 2. In Fig. 2, black circles represent previous stations taken by the Japanese (Uyeda et al., 1962, Yasui et al., 1963, Lee and Uyeda, 1965). Where the conductivity value was only estimated, the heat-flow values in microcal/cm^{2}sec are given with only one figure after the decimal point whereas when the conductivity was measured on the core by the needle probe method two figures after the decimal were used. Underlined stations indicate partial penetration. A letter J is attached for the stations taken with the Japanese instrument. As can be seen in Fig. 2, measurements made with the Scripps and the Japanese instruments fit well together although no stations were observed with both types of instruments.

The thermal conductivity values are shown for each station in Fig. 3 and in Table 1. Again three figures are for the measured values and two figures are for the estimated. The estimation was made arbitrarily from the nearby measured values. In estimating the conductivity values used for heat-flow computation, *in situ* values were disregarded as stated above. In Fig. 3, the *in situ* conductivity is marked by an asterisk. For the stations with *in situ* measurements, two conductivity values are given: one is the *in situ* value and the other is the value estimated from nearby measurements. It may be observed that the *in situ* values tend to be higher than the values obtained by the conventional measurements. The average of 11 core values of K is 1.94×10^{-3}, whereas the average of 10 *in situ* values, K_i, is 2.38×10^{-3}. The difference is about 20%. At station No. 54 both measurements were made to give $K=1.86\times10^{-3}$ for the measurement on the gravity core aboard the ship and $K_i=2.55\times10^{-3}$ for the *in situ* measurement. The difference amounted to 32%. If this difference is real, i.e. if the conductivity *in situ* is about 20–30% higher than that measured on core specimens, the consequence upon oceanic heat-flow in general is rather grave. However, to find out which of the two methods gives the best value of conductivity, more experiments are needed. Until then, we do not have reasons good enough for taking one and rejecting the other. However, the new and the old data should be mutually more consistent if the lower value of conductivity rather than the *in situ* one is used for computing the heat-flow at all stations. Accordingly, although both values are given in Table 1 for the stations where the conductivity has been measured *in situ*, the

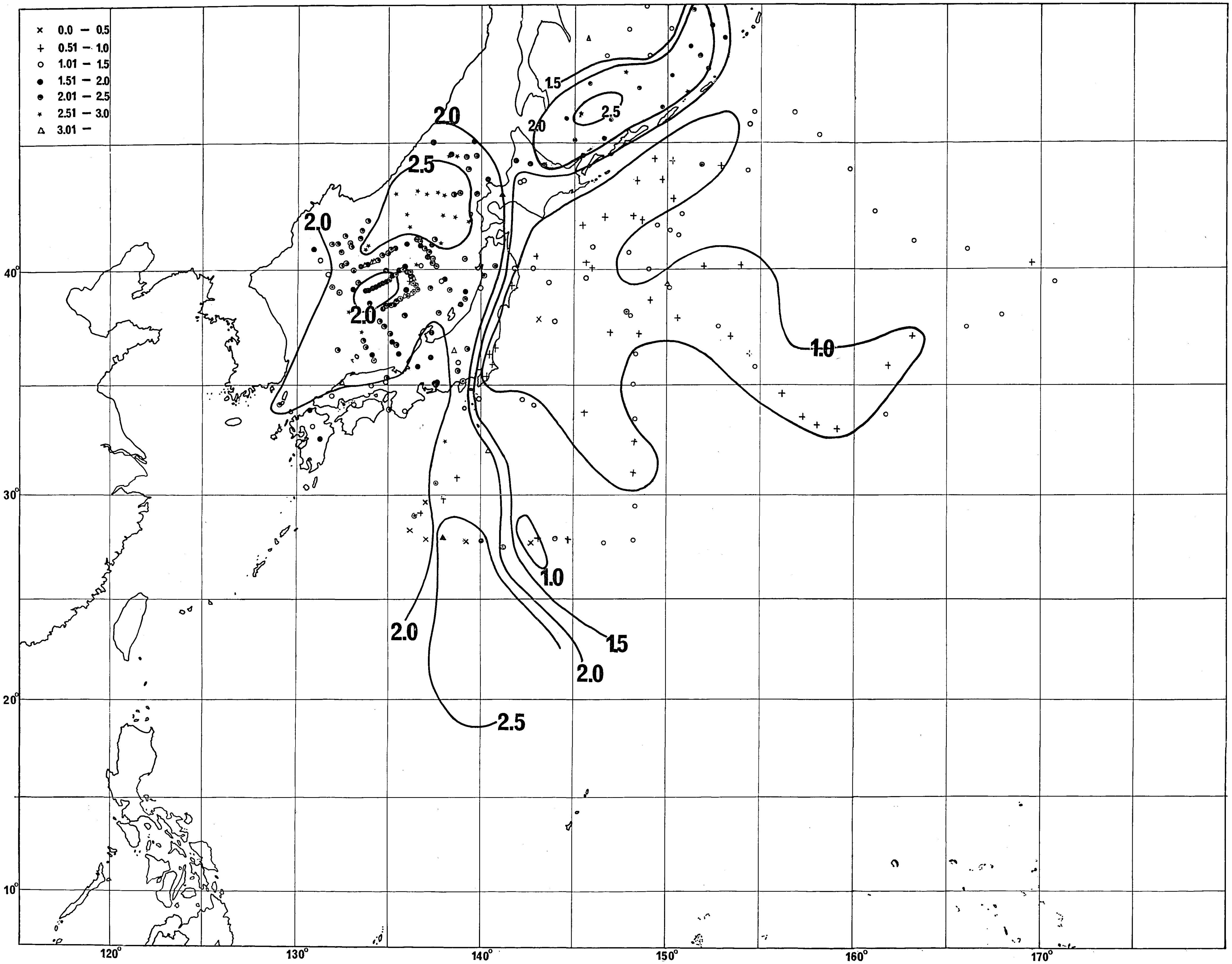

Fig. 4. Summary of heat-flow distribution in the northwestern Pacific and related areas. Data are due to Uyeda and Hôrai (1964), Yasui et al. (1966, a, b) and the present work.

heat-flow values in Fig. 2 are the ones computed from the conductivity values obtained from the conventional measurements only.

In Fig. 4, heat-flow values in the northwestern Pacific, the Japan Sea, the Sea of Ohotsk and the land of Japan are summarized. Because of the high density of stations in some area, heat-flow values are represented by symbols. Data in the Japan Sea and the Sea of Ohotsk are due to Yasui et al., (1966, a and b) and the land data are due to Uyeda and Hôrai, (1964). Tentative contours have been drawn in Fig. 4, but they have been influenced to a certain extent by the unpublished data by Dr. Langseth, Lamont Geological Observatory. Lamont data are not shown in Fig. 4.

In Figs. 2 and 4, the most remarkable feature in the area seaward of the island arc is the uniformity of the heat-flow. The average value of the heat-flow in the area seaward of the trench axis, as indicated by the dotted line in Fig. 2, is 1.15 ± 0.37 microcal/cm^{2}sec.

There were two previous high heat-flow stations at 39°22′N, 150°03′E and 38°12′N, 147°55′ giving 3.30 and 2.05 microcal/cm^{2}sec. But these localities were found this time to have slightly subnormal heat-flow. Whether these previous stations were in error or they represented very locally high heat-flow is not clear. In the first leg, uniformly subnormal heat-flow was found over the Northwest Pacific Rise and the Emperor Seamounts. It seems, therefore that geothermally these topographic highs are not the same as the East Pacific Rise on the other side of the Pacific Ocean which showed pronounced high heat-flow (von Herzen and Uyeda, 1963).

Immediately west of the Izu-Bonin Arc, the heat-flow is very different from place to place, suggesting the existence of anomalies of small areal extent which are not well defined by the present density of stations. Averaging the previously published values with the heat-flow values obtained on the Zetes cruise we get 1.73 ± 0.93 microcal/cm^{2}sec for the heat-flow along a strip about 250 km wide just west to the axis of the Izu-Bonin Arc. This value is higher that the heat-flow in the Pacific Basin east of the island arc which was 1.15 ± 0.37 microcal/cm^{2}sec. Moreover, the data suggest that the heat-flow high on the Izu-Mariana Arc may be an extention of the high heat-flow zone of Central Honshu, as suggested by the 2 microcal/cm^2 sec contour in Fig. 4. Fig. 5 is the observed heat-flow profile across the Izu-Bonin (Mariana) Ridge.

Still further west of the Izu-Mariana Ridge, in the Shikoku Basin, the heat-flow values we obtained were rather low. However, as mentioned

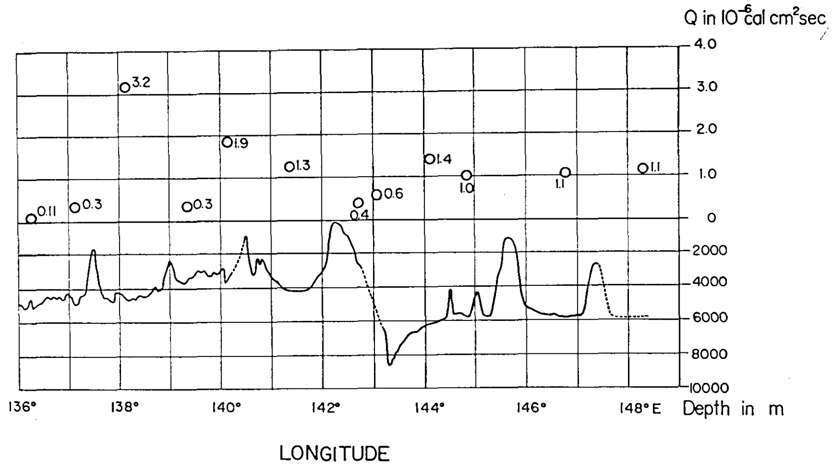

Fig. 5. Topographic and heat-flow profiles over the Izu-Bonin Arc at about 27°N.

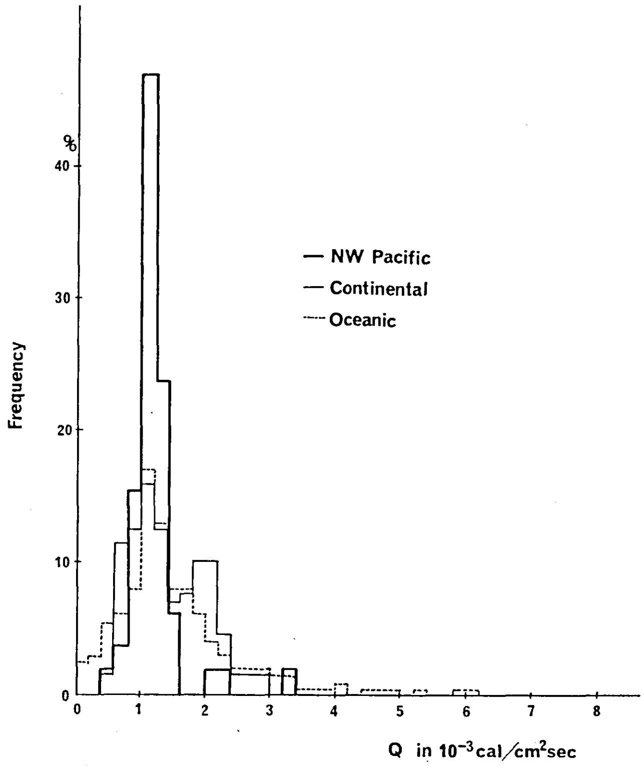

Fig. 6. Histogram of heat-flow values in the northwestern Pacific basin. For reference, histograms of the world's continents and oceans (Lee and Uyeda, 1965) are also shown.

above, Dr. M. Langseth of the Lamont Geological Observatory, Columbia University has provided us with their unpublished preliminary heat-flow values in this area. Their data show that in the Shikoku Basin the heat-flow is variable, there being both high and low values. Thus, although geographically the Shikoku Basin occupies a similar position with respect to its island arc as the Seas of Japan and Ohotsk, the distribution of heat-flow over its area is different from the rather uniformly elevated heat-flow in these seas as described by Yasui et al., (1966 a and b). At present the heat-flow in the Shikoku Basin cannot be contoured because of the sparseness of the data.

Fig. 6 shows the histogram of heat-flow values in the northwestern Pacific Basin seaward of the Trench axis. For reference, histograms of heat-flow values in the continental and oceanic area of the world taken from Lee and Uyeda (1965) are also shown. It can be clearly seen that the NW Pacific Basin generally has highly uniform and subnormal heat-flow. Modal value does not seem to be smaller than that of the world's oceans and continents, but higher values are notably few in the NW Pacific.

Our cruise provides additional factual information on heat-flow in and near the island arc of Japan. In Fig. 7a and 7b heat-flow values are plotted against the distance from the axis of the trench for the Kuril, Honshu and Izu-Bonin Arc. For the Kuril Arc recent data in the Sea of Ohotsk of Yasui et al., (1966, a) were used. For the Honshu Arc, the data in the Sea of Japan were taken from Yasui et al., (1966 b). In order to show the general trend more clearly, in Fig. 7b, heat-flow values of Fig. 7a are averaged for every 100 km interval to get the hollow circles from which the smooth curves were drawn. It may be observed that the heat-flow tends to get slightly lower near the axis of the trench. Inside the trench, heat-flow, via a minimum at about 100 km landward from the trench axis, becomes high. This high heat-flow persists all through the Japan Sea in the case of the Honshu Arc. In the Kuril Arc, heat-flow becomes lower in the part of the Sea of Ohotsk more than 200 km away from the trench axis. In the case of the Izu-Bonin Arc, heat-flow values scatter much and the distribution is irregular. These differences in the distribution of heat-flow may be related to the fundamental processes of formation of these island arcs and marginal seas.

The uniform and somewhat low heat-flow in the northwestern Pacific Basin is in sharp contrast with the generally high and non-uniform heat-

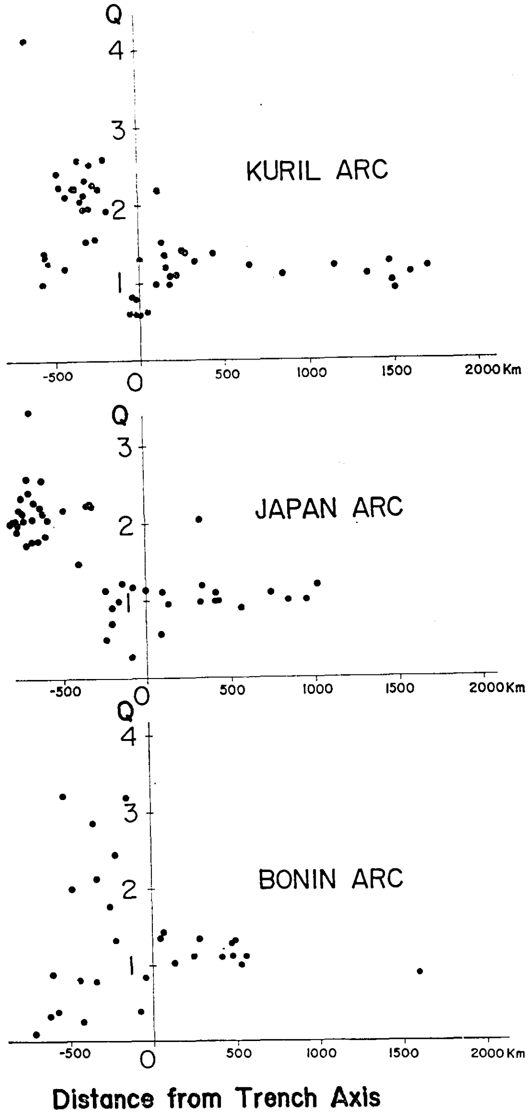

Fig. 7. a. Heat-flow values plotted against the distance from the trench axis for Kuril, Honshu and Izu-Bonin Arcs, Heat-flow value Q is in microcal/cm^2 sec.

flow off the shores of North and Central America (Vacquier, 1966). The mean value of heat-flow in this somewhat larger area is about twice what it is in the northwestern Pacific Basin. This macroscopic anomaly is indeed welcome for those who imagine the Earth's mantle as being

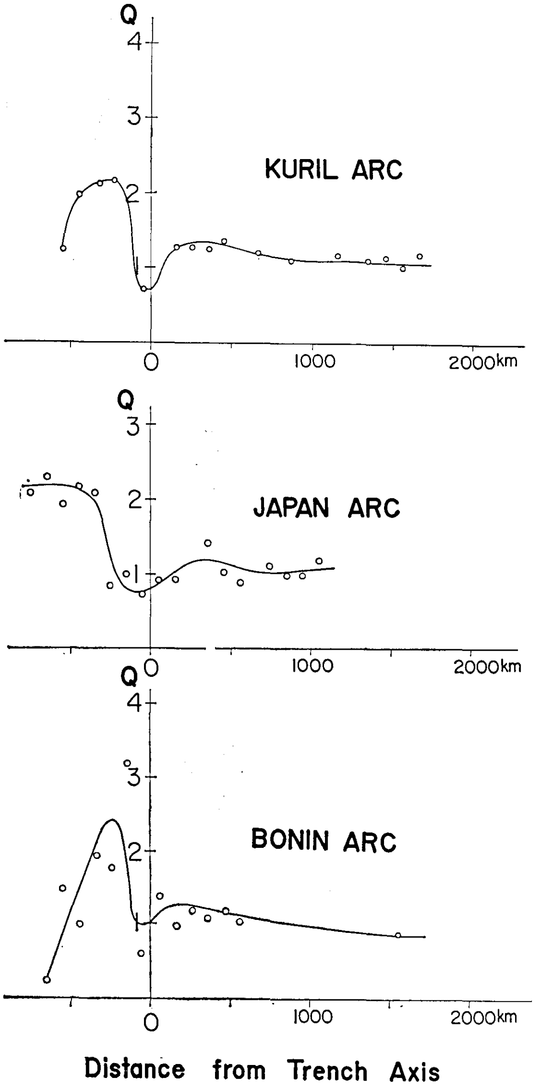

Fig. 7. b. Averaged heat-flow values in 100 km intervals from the trench axis for the three arcs.

extruded in the Eastern Pacific over the East Pacific Rise, the Cocos, Carnegie and Tehuantepec Ridges as well as under the western part of the North American Continent. The Western Pacific would then be the place where the crust and upper mantle would gradually sink. The presence of the Emperor Seamount Ridge and Shattsky (NW Pacific) Rise which were imagined by some to be tectonically active areas (Vening

Meinesz, 1964, p. 88) complicated the situation and made this interpretation less likely. But now that we know that these features are not only inactive at the present time because of low seismicity, but that they have been so long enough to be geothermally cold, makes the East Pacific Rise and its associated ridges the only large active tectonic features in the northern half of the Pacific Ocean.

Acknowledgement: This work was supported by the Office of Naval Research, the National Science Foundation and the Japanese Society of Promotion of Science under the US-Japan Cooperative Science Program. The authors are grateful to the Captain A. Phinney and Crew of R/V ARGO. We should mention the assistance rendered by E. Silver, F. Dixon, J. Lawson, A. Raff of Scripps Institution of Oceanography, G. Converse, Y. Fukao, M. Nishikawa, K. Sudo, M. Kimura, and M. Inoue of the University of Tokyo, T. Sato, Hydrographic Department, H. Akamatsu and K. Hata, Japan Meteorological Agency. Mrs. Y. Tomoda and Miss T. Tanaka are acknowledged for their help in preparation of the manuscript and figures. Profs. C. Tsuboi and T. Rikitake are acknowledged for their interest and encouragement.

References

LEE, W. H. K., and S. UYEDA, (1965) "Review of Heat Flow Data" in *Terrestrial Heat Flow*, pp. 87-190, Geophys. Monograph., No. 8, American Geophys. Union.

UYEDA, S. and K. HÔRAI, (1964) "Terrestrial Heat Flow in Japan," *J. Geophys. Res.*, **69**, 2121-2141.

UYEDA, S., K. HÔRAI, M. YASUI, and H. AKAMATSU, (1962), "Heat Flow Measurements over the Japan Trench," *J. Geophys. Res.*, **67** (3), 1186-1188.

UYEDA, S., Y. TOMODA, K. HÔRAI, H. KANAMORI and H. FUTI, (1961), "Studies of the Thermal State of the Earth, the 7th paper, A Sea Bottom Thermogradmeter," *Bull. Earthq. Res., Inst.*, **36**, 115-131.

VAQUIER, V., (1966), "Heat Flow in the Eastern Pacific Ocean," to be published in *Bull. Earthq. Res., Inst.*

VENING MEINESZ, F. A., (1964), *The Earth's Crust and Mantle*, Elsevier.

VON HERZEN, R. P., and A. E. MAXWELL, (1959), "The Measurements of Thermal Conductivity of Deep-sea Sediments by a Neddle Probe Method." *J. Geophys. Res.*, **64**, 1557-1565.

VON HERZEN, R., P., A. E. MAXWELL and J. M. SNODGRASS, (1962), "Measurement of Heat Flow through the Ocean Floor," *Symposium, Temperature*, 4th, pp. 769-777, Reinhold Publishing Coorporation, New York.

VON HERZEN, R. P., and S. UYEDA, (1963), "Heat Flow through the Eastern Pacefic Ocean Floor," *J. Geophys. Res.*, **68**, 4219-4250.

YASUI, M., K. HÔRAI, S. UYEDA and H. AKAMATSU, (1963), "Heat Flow Measurement in the Western Pacific during the JEDS-5 and other Cruises in 1962 aboard M/S Ryofu Maru," *Oceanogr. Mag.*, **14**, (2), 147-156.

YASUI, M., T. KISHII, M. HASHIMOTO and K. SUDÔ, (1966, a), "Preliminary Report on Heat Flow in the Sea of Ohotsk," read before the 11th Pacific Congress, Tokyo.

YASUI, M. and T. WATANABE, (1965), "Studies of theThermal State of the Earth, The 16th Paper: Terrestrial Heat Flow in the Japan Sea (I).," *Bull. Earthq. Res. Inst.*, **43**, 549-563.

YASUI, M., T. WATANABE, T. KISHII and S. UYEDA, (1966, b), "Studies of the Thermal State of the Earth, The 18th Paper, Terrestrial Heat Flow in the Japan Sea (II)." *Bull. Earthq. Res. Inst.*, **44**, This issue.

---

73. 地球熱学　第19報　北西太平洋海域の地殻熱流量

スクリプス海洋研究所　Victor VACQUIER
地震研究所　上田誠也
舞鶴海洋気象台　安井正
スクリプス海洋研究所　John SCLATER, Charles CORRY
東京大学大学院　渡部暉彦

日米協力太平洋研究の一環として行なわれた，Argo 号(スクリプス研)による Zetes 航海において，65点の熱流量測定が行なわれた．測定海域は，北西太平洋であり，北西太平洋海丘，天皇山脈海域を含む．海溝より海側の北西太平洋海盆は一様な熱流量分布をもち，平均は $1.15 \pm 0.37 \times 10^{-6}$ cal/cm^2 sec である．この値は，東南太平洋海域での平均値の略 1/2 である．伊豆-マリアナ弧では高流量が観測されたが，四国海盆は，必ずしも高熱流量を示さないようである．この点で，四国海盆は，日本海，オホーツク海などの内陸海とは異なつている．本観測において，はじめて，海底底質土の熱伝導度を，海底現場において測定することに成功した．その結果，現場法による熱伝導度は，従来の測定法によるものよりも20%程度大きな値を示した．この差が，有意差であれば，従来の海洋地域の熱流量測定値は一様に20%程度高く再評価されるべきであることになる．この問題は重要なので，さらに詳しい研究を必要とする．本論文では，一応，従来の測定法による熱伝導度を用いて熱流量が計算された．